Electronic Supplementary Material (ESI) for Journal of Materials Chemistry A.

A sulfur-containing polymer-plasticized poly(ethylene oxide)-based electrolyte enables highly efficient lithium dendrite suppression

Zhenying Chen,[a] Jingyan Li,[ab] Feng Qiu,[a] Chenbao Lu,[a] Jinhui Zhu*[a] and Xiaodong Zhuang*[a]

[a]*The meso-Entropy Matter Lab, State Key Laboratory of Metal Matrix Composites, School of Chemistry and Chemical Engineering, Frontiers Science Center for Transformative Molecules, Shanghai Jiao Tong University, Shanghai 200240, China*
E-mail: zhujinhui1109@sjtu.edu.cn, zhuang@sjtu.edu.cn

[b]*College of Chemistry and Molecular Engineering, Zhengzhou University, Zhengzhou, 450001, Henan, China*

Synthesis of Sultine [1]

Sodium hydroxymethanesulfinate dihydrate (29.2 g, 247.3 mmol) and tetrabutylammonium bromide (12.21 g, 37.9 mmol) were added to DMF (100 mL) solution of 1,2-bis(bromomethyl)benzene (10 g, 37.9 mmol). The mixture was stirred at 0 °C under Ar for 2 h, and then, water (200 mL) was added. After removal of solid by filtration, the filtrate was extracted with ether, dried with anhydrous magnesium sulfate, and removal of solvent. The crude product was purified by a silica gel column chromatography. Elution of the column with 14% EtOAc–petroleum ether gave the oil product. ^{1}H NMR (500 MHz, $CDCl_3$): δ (ppm) 7.19-7.42 (m, 4H), 5.31 (d, 1H), 4.97 (d, 1H), 4.42 (d, 1H), 3.55 (d, 1H).^{13}C NMR (500 MHz, $CDCl_3$): δ (ppm) 56.9, 63.0, 125.7, 126.2, 127.8, 129.6, 133.7.

Synthesis of S-containing polymer (SCP)

Sultine (0.4 g) was added to a 50 mL Schlenk flask under inert atmosphere, and heated to 80 °C for 15 h. Afterwards, sublimed sulfur (1 g) was added to the flask under inert atmosphere. The mixture was further stirred for 1 h at 180 °C, the black product was taken out until cooling to room temperature. Then, the SCP was obtained by washing the black product three times with CS_2.

Preparation of PEO-based composite polymer electrolytes

Under Ar atmosphere, the SCP was added into 25 mL anhydrous acetonitrile and stirred for 2 h. Then, PEO (1 g, MW = 600000 g mol^{-1}) and LiTFSI (326 mg) was added into the above solution and stirred for 12 h. The resulting solution was poured onto a polytetrafluoroethylene plate, followed by drying under vacuum for 12 h at 50 ℃. In addition, PEO and LiTFSI need to be dried in vacuum before using.

Preparation of cathode electrode

The $LiFePO_4$ and $LiNi_{0.8}Mn_{0.1}Co_{0.1}O_2$ cathodes were prepared by mixing $LiFePO_4$/ $LiNi_{0.8}Mn_{0.1}Co_{0.1}O_2$, super-P, PVDF in NMP with a weight ratio of 80: 10: 10. The slurry was coated to Al foil and dried at 80 °C under vacuum. The loading of the active material is ~1 mg cm^{-2}.

Materials Characterization

X-ray diffraction (XRD) analysis was conducted with an X-ray diffractometer using Cu Kα radiation (λ= 0.154056nm). The data were recorded in the range of 5-80^{o} with 6^{o}/min. SEM images were acquired by scanning electron microscope (SEM, FEI Nova NanoSEM 450, 15 kV). The X-ray photoelectron spectroscopy (XPS) analysis was performed using a Kratos Axis UltraDLD spectrometer (AXIS ULTRA DLD, Kratos Analytical Ltd., UK) with monochromatic Al Ka source (1486.6 eV). TGA was performed with a Discovery TGA550 thermobalance a heating rate of 20 °C min^{-1} under N_2 atmosphere. Differential scanning calorimetry (DSC) was carried out in the Q2000 (TA instruments) from -80 °C to 150 °C with a heating rate of 10 °C min^{-1}. Fourier transform infrared (FTIR) spectroscopy was measured on Spectrum 100 (Perkin Elmer) by preparing KBr pellets. Raman spectra were obtained using DXR Raman Spectrometer (ThermoFisher) equipped with a 532 nm wavelength laser. Gel permeation chromatography (GPC) was performed on HLC-8320GPC with THF as an eluent. The ^{1}H NMR and ^{13}C NMR spectroscopies were conducted on a Bruker 600 MHz spectrometer at room temperature. Solid-state magic–angle–spinning ^{13}C NMR experiments were performed on a Bruker AVANCE III 600 WB spectrometer with the operating frequency of 150.12 MHz. Solid–state magic–angle–spinning (MAS) ^{7}Li NMR measurements are recorded on a Bruker Avance NEO 600 MHz NMR spectrometer at 14.09 T with the operating frequency of 233.2 MHz (^{7}Li). ^{7}Li NMR spectra are acquired using a 3.2 mm DVT HXY MAS NMR probe. ^{7}Li chemical shift is referenced to solid LiCl at −1.1 ppm.

Electrochemical measurements

The Li^{+} ionic conductivity was measured by electrochemical impedance spectroscopy (EIS) with stainless steel (SS) as electrodes in the range of 10^{5}–0.01 Hz.

The ionic conductivity was obtained using the following equation (1):

$$\sigma = \frac{L}{R_b S} \quad (1)$$

where L is the thickness of the electrolyte membrane, R is the bulk resistance and S is

the contact area of the electrode and electrolyte.

The electrochemical stability window of the electrolytes was evaluated via linear sweep voltammetry (LSV) in the potential range from 2.5 to 5.5 V at a scanning rate of 1 mV s^{-1} with a stainless steel as working electrode and Li metal as a reference and counter electrode.

The Li^+ transference number (t^+) of electrolyte was measured in symmetric Li|Li cell with DC polarization of 10 mV. The t^+ was then calculated using equation (2):

$$t_{Li^+} = \frac{I_{SS}(\Delta V - I_0 R_0)}{I_0(\Delta V - I_{SS} R_{SS})} \quad (2)$$

where I_0 and I_{ss} are the initial and stable currents during polarization, and R_0 and R_{ss} are the resistance of the solid electrolyte before and after polarization.

EIS, LSV and chronoamperometry tests were conducted at CHI660E electrochemical work station at 60 ℃.

Symmetric Li|Li cells, Li|$LiFePO_4$ and Li|NCM811 full cells were assembled in Ar-filled glovebox, and tested on battery test system (LAND-CT2001C).

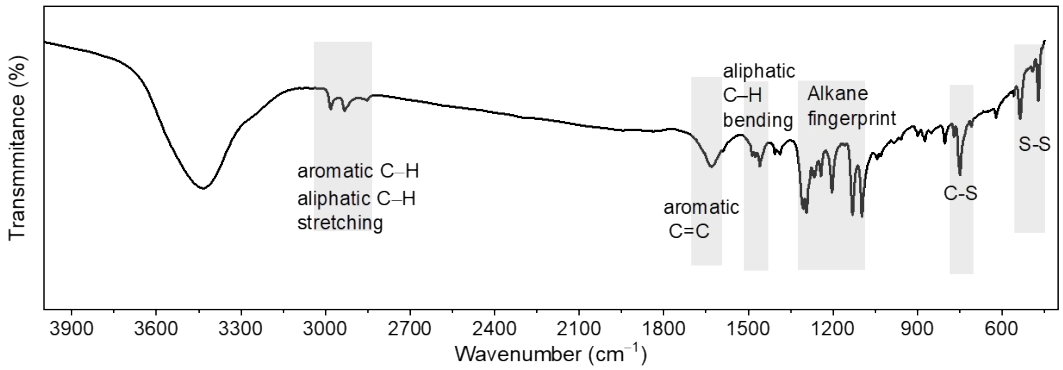

Fig. S1. FTIR spectra of SCP.

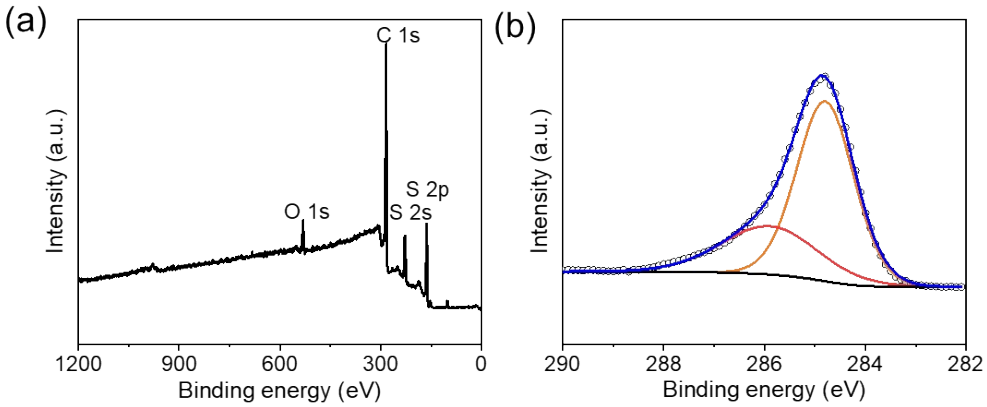

Fig. S2. XPS survey (a) and C 1s XPS (b) spectra of SCP.

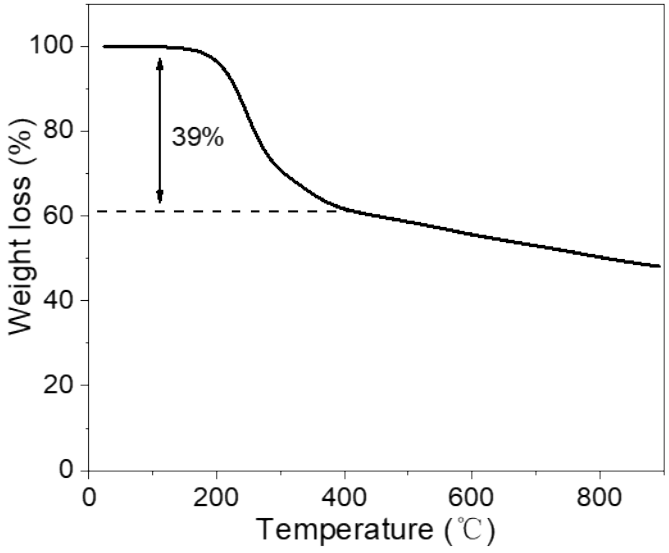

Fig. S3. TGA curve of SCP.

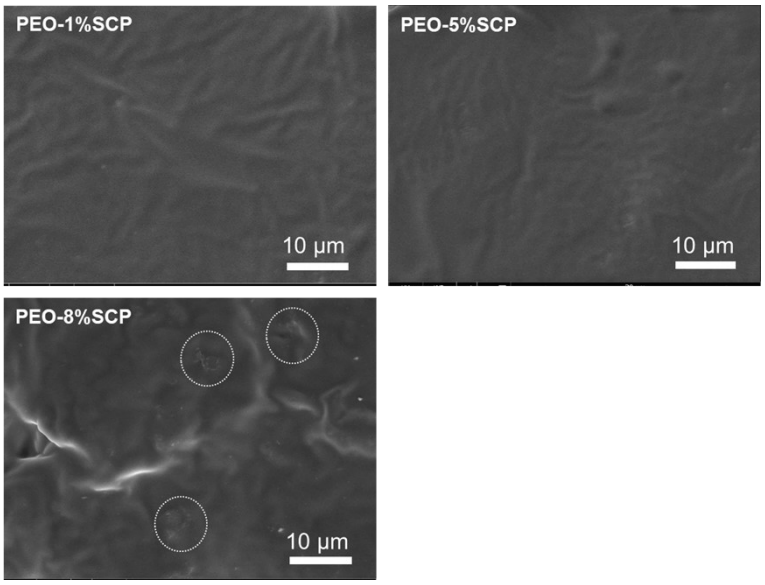

Fig. S4. SEM images of surface of PEO-5%SCP electrolyte.

Fig. S5. Optical photographs of as-prepared solid electrolyte membranes.

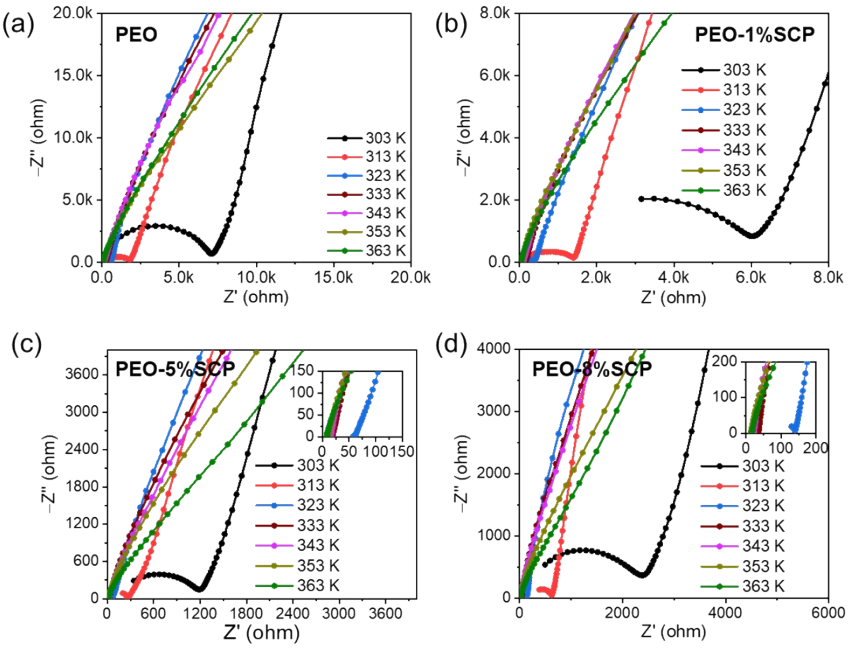

Fig. S6. EIS spectra of SS|SS cells with as-prepared solid electrolytes at different temperature.

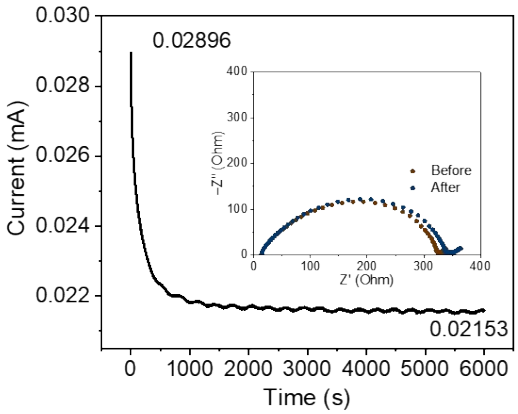

Fig. S7. The i-t curves of Li|Li cell with PEO electrolyte (inset: EIS spectra before and after chronoamperometry test).

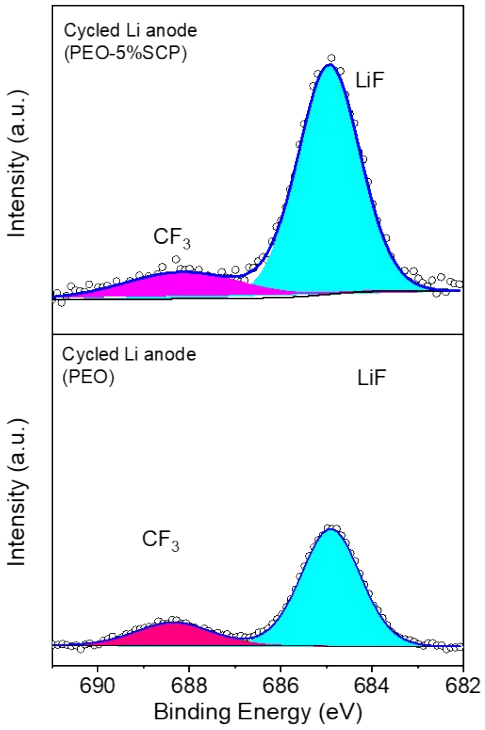

Fig. S8. F 1s XPS spectra of cycled Li anode (PEO-5%SCP) and (PEO).

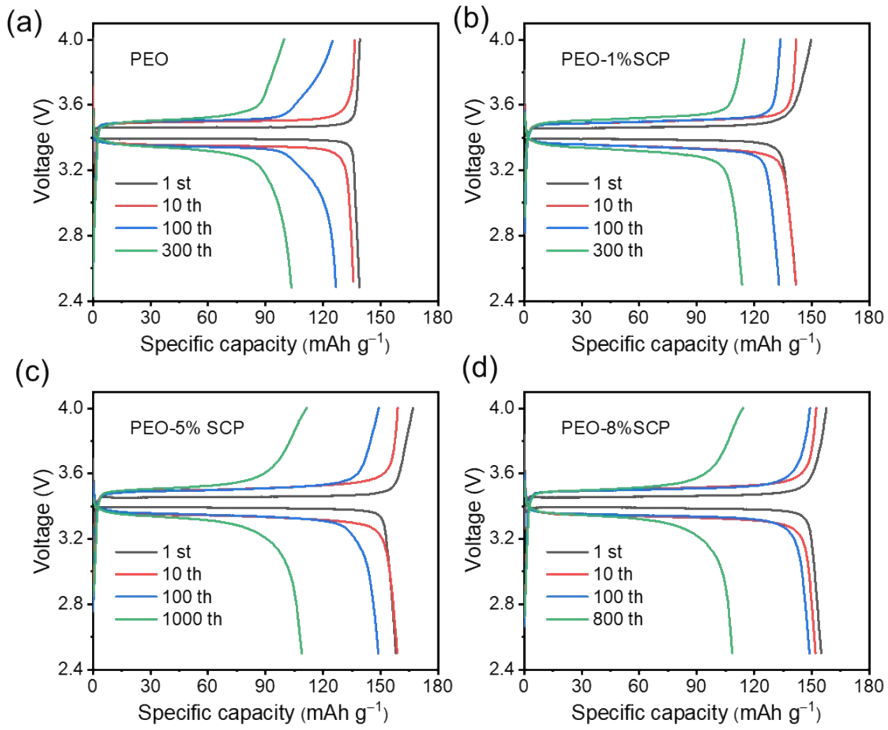

Fig. S9. The GCD curves of Li|$LiFePO_4$ cells with as-prepared solid electrolytes.

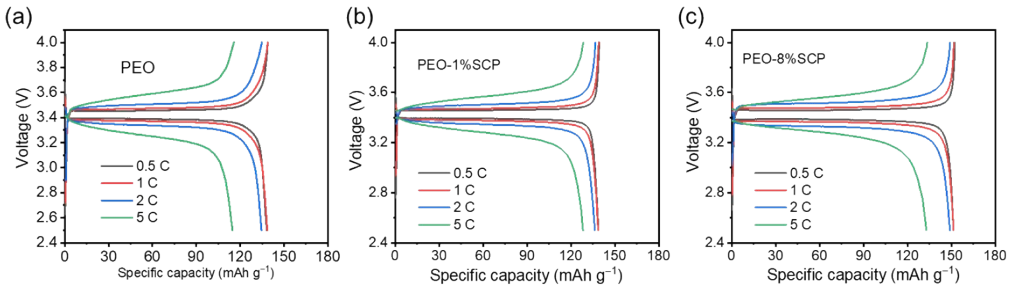

Fig. S10. The GCD curves of Li|$LiFePO_4$ cells at various C-rates.

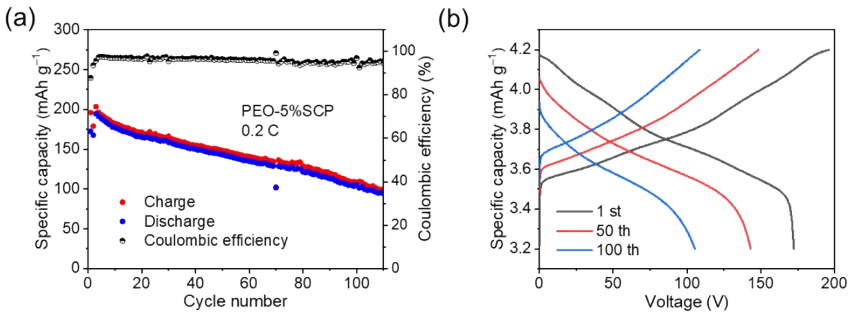

Fig. S11. Cycling performance (a) and GCD curves (b) of Li|NCM811 cell with PEO-5%SCP electrolyte.

Table S1 The crystallinities of as-prepared solid electrolytes.

Electrolytes	PEO	PEO-1%SCP	PEO-5%SCP	PEO-8%SCP
χ_c	39.7	32.9	30.9	34.2

The crystallinity (χ_c) of the composite polymer electrolyte was calculated by formula (3):

$$\chi_c = \frac{\Delta H_f}{\Delta H_{PEO}} \times 100\% \quad (3)$$

Where ΔH_f is the fusion enthalpy of electrolyte, and the value of ΔH_{PEO} is 203 J g^{-1} for the perfect crystal by the ideal fusion method for the melting enthalpy of 100% crystalline PEO. [2]

Table S2 The ionic conductivities (S cm^{-1}) for the as-prepared solid electrolytes.

	303 K	313 K	323 K	333 K	343 K	353 K	363 K
PEO	7.29×10^{-7}	2.82×10^{-6}	8.71×10^{-6}	2.35×10^{-5}	4.36×10^{-5}	6.22×10^{-5}	9.11×10^{-5}
PEO-1%SCP	8.50×10^{-7}	3.64×10^{-6}	1.28×10^{-5}	3.40×10^{-5}	5.67×10^{-5}	8.50×10^{-5}	1.21×10^{-4}
PEO-5%SCP	4.25×10^{-6}	1.89×10^{-5}	8.50×10^{-5}	2.43×10^{-4}	4.25×10^{-4}	5.67×10^{-4}	7.09×10^{-4}
PEO-8%SCP	2.13×10^{-6}	8.10×10^{-5}	3.62×10^{-5}	1.42×10^{-4}	2.22×10^{-4}	2.55×10^{-4}	3.00×10^{-4}

Table S3 Calculation of lithium transference numbers of PEO and PEO-5%SCP electrolytes

	V (mV)	I_s (mA)	I_0 (mA)	R_s (Ω)	R_0 (Ω)	I_0*R_0	I_s*R_s	t^+
PEO	10	0.0216	0.0289	335	312	9.0168	7.236	0.265864
PEO-5%SCP	10	0.0267	0.03779	340	250	9.4475	9.078	0.423385

Table S4 elemental analysis for cycled Li anodes and electrolytes by XPS.

Cycled Li anode (PEO)						
Element	C	N	O	F	S	Li
Content	12.65	0.10	28.8	0.30	0.10	58.08
Cycled Li anode (PEO-5%SCP)						
Element	C	N	O	F	S	Li
Content	8.27	0.37	28.87	0.47	0.55	61.48
Fresh PEO-5%SCP membrane						
Element	C	N	O	F	S	Li
Content	63.96	1.86	21.73	7.42	3.03	2
Cycled PEO-5%SCP membrane						
Element	C	N	O	F	S	Li
Content	66.84	1.74	11.05	9.2	2.84	8.33

Table S5 Comparison of the electrochemical properties of cells with PEO-5%SCP electrolyte and reported CPEs.

Filler types	**Ionic conductivity (S cm^{-1})**	**Lithium transference numbers**	**Battery performance ($LiFePO_4$/Li cell)**	
Ca–CeO_2	1.3 × 10^{-4}/60 °C	0.453/60℃	93 mAh g^{-1} after 200 cycles/1 C/60℃	[3]
Black phosphorus	2 ×10^{-4} 60 °C	0.4/60℃	112.5 mAh g^{-1} after 200/0.1 mA cm^{-2}/60℃	[4]
LLTO-nanowire	3.63 × 10^{-4}/60 °C	0.195/60℃	123 mAh g^{-1} after 100 cycles/0.5C/60℃	[2]
g-C_3N_4 nanosheets	1.52 × 10^{-4}/60 °C	0.56/60℃	155 mAh g^{-1} after 100 cycles/0.2C/60℃	[5]
ZIF-8	2.2 × 10^{-5}/30 °C	0.36/60℃	111 mA·h g^{-1} after 350 cycles/0.5 C/60℃	[6]
UIO/Li- ionic liquid	1.3 × 10^{-4}/30 °C	0.35/30℃	144 mAh g^{-1} after 100 cycles/0.5C/60℃	[7]
TiO_2@PDA	4.36 × 10^{-4}/55 °C	0.19/55 °C	125.5 mAh g^{-1} after 150 cycles/1C/55℃	[8]
GO- ionic liquid	1.8 × 10^{-5}/25℃	/	127.6 mAh g^{-1} after 100 cycles/0.1C/60℃	[9]
This work	2.43 × 10^{-4}/60 °C	0.42/60℃	136.7 mAh g^{-1} after 300 cycles/1C/60℃; 108.9 mAh g^{-1} after 1000 cycles/1C/60℃	

Table S6 Resistance of Li‖$LiFePO_4$ cells with PEO and PEO-5%SCP electrolytes.

PEO/PEO-5%SCP	initial	After 2 cycles	After 50 cycles
R_b (Ω)	16.95/13.63	19.28/8.267	15.61/15.72
R_{SEI} (Ω)	38.74/36.78	55.34/46.06	89.2/24.82
R_{ct} (Ω)	36.63/12.84	36.79/32.54	78.92/51.74

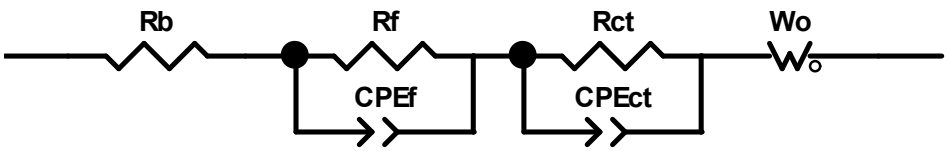

Schematic illustration of the equivalent circuit models for EIS spectrum fitting of Li‖$LiFePO_4$ cells before and after cycles. R_b represent the sum of bulk resistance. R_f (R_{SEI}) and R_{ct} are the interface resistance and charge transfer resistance, respectively. W represent the Warburg diffusion element.

References

[1] M.D. Hoey, D.C. Dittmer, J Org Chem, 56 (1991) 1947-1948.
[2] L. Zhu, P. Zhu, Q. Fang, M. Jing, X. Shen, L. Yang, Electrochimica Acta, 292 (2018) 718-726.
[3] H. Chen, D. Adekoya, L. Hencz, J. Ma, S. Chen, C. Yan, H. Zhao, G. Cui, S. Zhang, Advanced Energy Materials, 10 (2020).
[4] N. Wu, Y.T. Li, A. Dolocan, W. Li, H.H. Xu, B.Y. Xu, N.S. Grundish, Z.M. Cui, H.B. Jin, J.B. Goodenough, Adv Funct Mater, 30 (2020) 2000831.
[5] Z. Sun, Y. Li, S. Zhang, L. Shi, H. Wu, H. Bu, S. Ding, Journal of Materials Chemistry A, 7 (2019) 11069-11076.
[6] Z. Lei, J. Shen, W. Zhang, Q. Wang, J. Wang, Y. Deng, C. Wang, Nano Res, 13 (2020) 2259-2267.
[7] J.-F. Wu, X. Guo, Journal of Materials Chemistry A, 7 (2019) 2653-2659.
[8] E. Zhao, Y. Guo, A. Zhang, H. Wang, G. Xu, Nanoscale, 14 (2022) 890-897.
[9] Z. Hu, X. Zhang, J. Liu, Y. Zhu, Front Chem, 8 (2020) 232.